ACS OMEGA

Article

Cite This: ACS Omega 2017, 2, 6691-6702

http://pubs.acs.org/journal/acsodf

Mechanistic Insights into the Differential Catalysis by RheB and Its Mutants: Y35A and Y35A-D65A

Chaithanya Kotyada,*[,†] Aditi Maulik,[†] Anand Srivastava,[†] and Mahavir Singh*[,†,‡]

[†]Molecular Biophysics Unit and [‡]NMR Research Centre, Indian Institute of Science, Bengaluru 560012, India

Supporting Information

ABSTRACT: RheB GTPase is a Ras-related molecular switch, which regulates the mTOR signaling pathway by cycling between the active [guanosine triphosphate (GTP)] state and inactive [guanine diphosphate (GDP)] state. Impairment of GTPase activity because of mutations in several small GTPases is known to be associated with several cancers. The conventional GTPase mechanism such as in H-Ras requires a conserved glutamine (Q64) in the switch-II region of RheB to align the catalytic water molecule for efficient GTP hydrolysis. The conformation of this conserved glutamine is different in RheB, resulting in an altered conformation of the entire switch-II region. Studies on the atypical switch-II conformation in RheB revealed a distinct, noncanonical mode of GTP hydrolysis. An RheB mutant Y35A was previously shown to exclusively enhance the intrinsic GTPase activity of RheB, whereas the Y35A-D65A double mutant was shown to reduce the elevated GTPase activity. Here, we have used all-atom molecular dynamics (MD) simulations for comprehensive understanding of the conformational dynamics associated with the fast (Y35A) and slow (Y35A-D65A) hydrolyzing mutants of RheB. Using a combination of starting models from PDB structures and in-silico generated mutant structures, we discuss the observed conformational deviations in wild type (WT) versus mutants. Our results show that a number of interactions of RheB with phosphates of GTP as well as Mg^{2+} are destabilized in Y35A mutant in the switch-I region. We report distinct water dynamics at the active site of WT and mutants. Furthermore, principal component analysis showed significant differences in the conformational space sampled by the WT and mutants. Our observations provide improved understanding of the noncanonical GTP hydrolysis mechanism adopted by RheB and its modulation by Y35A and Y35A-D65A mutants.

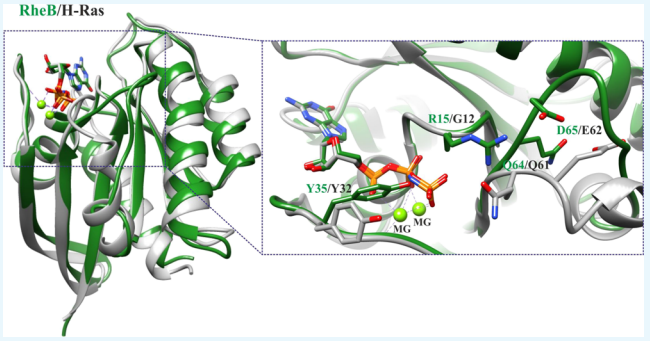

INTRODUCTION

Ras superfamily GTPases are guanine nucleotide binding proteins that function as "molecular switches" by cycling between guanine diphosphate (GDP)-bound "off" state and a guanosine triphosphate (GTP)-bound "on" state.[1−4] The large conformational changes accompanying these states are responsible for the regulation of multiple cellular processes.[2,5−8]

Members of this superfamily of GTPases share core G-domain architecture with highly conserved signature motifs (G1−G5) that are responsible for nucleotide binding and hydrolysis (Figure 1A). The G1 motif with a consensus sequence of GxxxxGKT/S stabilizes the phosphates of the nucleotide and is known as a P loop (Figure 1A). G2 has a single conserved Thr residue, whereas the consensus DxxG residues specify the G3 region. G2 and G3 motifs mediate large conformational changes following the transition from GTP to GDP state and vice versa and are known as switch-I and switch-II regions, respectively (Figure 1A). G4 (NKxD) and G5 (SAK) motifs together provide contacts required for the stabilization of the guanine base.[9,10]

Ras oncogenic mutations are known to hinder the conventional GTP hydrolysis process in GTPases, resulting in proteins showing an elevated activity in the cell.[11−14] Significant amount of work has been dedicated to elucidate the mechanism of GTPase reaction in Ras.[15−22] Studies have shown the imperative role of a conserved glutamine neighboring glycine of DxxG motif in switch-II of G3 region, to align a catalytic water molecule for GTP hydrolysis.[23,24] Also, the role of several conserved and nonconserved residues in the active site has been elucidated in the GTPase reaction.[11,24−30] Since the realization of the critical role of the conserved glutamine in GTP hydrolysis of Ras, leucine mutants of the same were widely used among the superfamily proteins as constitutively active forms to study their cellular functions.[11,31−33]

Ras homology enriched in brain (RheB), a member of the Ras superfamily GTPases, regulates protein translation and cellular growth by mediating signaling between tumor suppressor proteins TSC1,2 (tuberous sclerosis complex 1 and 2) and mTOR (mammalian target of rapamycin) complex 1.[34,35] Unlike other Ras family GTPases, the crystal structure of

Received: July 19, 2017
Accepted: September 28, 2017
Published: October 12, 2017

DOI: 10.1021/acsomega.7b01025
ACS Omega 2017, 2, 6691−6702

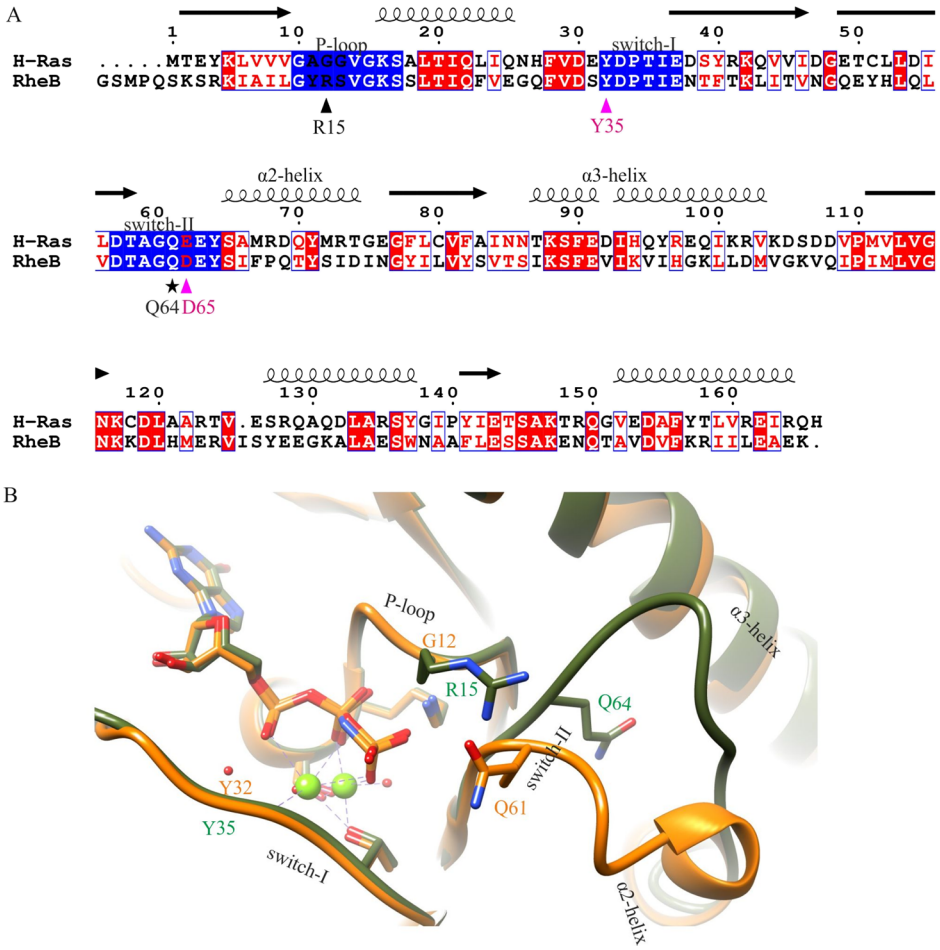

Figure 1. Comparison of H-Ras and RheB GTPases. (A) Sequence alignment of the crystal structures H-Ras (PDB ID 5P21) and RheB (PDB ID 4O25). (Conserved domains—dark blue, mutants in the current study—pink triangle, conserved catalytic glutamine—black star, critical arginine residue of P loop—black triangle). (B) Overlay of crystal structures H-Ras-GppNHp (orange) and RheB-GTP (dark green), representing the active site.

RheB shows that the conserved glutamine (Q64) of the switch-II region adopts a catalytically incompetent conformation[35] (Figure 1B). The rate of intrinsic hydrolysis in RheB was found to be unusually slow compared to Ras, and this was attributed to the alternate conformation of Q64.[35−37] Further, the glutamine to leucine mutation did not have any effect on the hydrolysis rates of RheB.[36] Extensive studies were performed on RheB to decipher its mode of hydrolysis and develop new strategies to control the GTP cycle. A noncanonical mode of GTP hydrolysis was proposed, which details the role of aspartic acid (D65) neighboring the conserved glutamine (Q64), as a potential water-aligning residue.[36] Additionally, Y35 of the switch-I region was shown to autoinhibit the intrinsic GTP hydrolysis of RheB as Y35A mutant exhibits an elevated hydrolysis rate.[36]

Here, we present an all-atom molecular dynamics (MD) simulation study of the wild type (WT), Y35A, and Y35A-D65A mutants of RheB. Our investigation provides the structural rationale toward the effects of mutations on the intrinsic hydrolysis of RheB GTPase. We report distinct dynamics at the active site region of RheB, which distinguishes it from conventional Ras family proteins. Further, these observations give molecular-level insights into the role of Y35 of switch-I and D65 of switch-II for the modulation of intrinsic GTP catalysis rates in RheB.

METHODS

Model Preparation. Crystal structures (PDB ID 4O25 B and 3SEA B) were used as starting structures for the generation of initial models for the simulations of RheB WT and RheB Y35A mutant, respectively. The guanosine 5′-[β,γ-imido]-triphosphate (GppNHp) nucleotide in the RheB Y35A mutant was replaced with a GTP molecule. The sequence of the GppNHp-bound RheB Y35A mutant (PDB ID 3SEA B) differs from the wild type (PDB ID 4O25 B) with a conservative K161R substitution toward the C-terminal (Figure S1A). Computer-aided Y35A and Y35A-D65A mutants were generated over the wild-type crystal structure using UCSF Chimera software package.[38] All models were stripped of crystallographic water molecules prior to system preparation. Table 1 shows the models and their representations followed in the text. Table 2 represents the production run times of all systems in the current work.

MD Simulations. All MD simulations were carried out with the GROMACS simulation package, version 5.0.4, using an all-atom CHARMM27 force field with CMAP correction and TIP3P rigid water model.[39] For simulations, each model was placed in a cubic box containing TIP3P water with a minimum distance of 10 Å between the protein atom and the box surface. Counter ions Na^+ and Cl^- were added for charge neutralization. Steepest descent energy minimization was used

DOI: 10.1021/acsomega.7b01025
ACS Omega 2017, 2, 6691−6702

Table 1. Models Used for MD Simulations[a]

model	PDB ID	template for modeling	representation
RheB wild-type crystal structure	4O25	4O25-B	RheB WT
RheB Y35A crystal structure	3SEA	3SEA-B	RheB Y35A-xtal
RheB Y35A model	not available	4O25-B	RheB Y35A-mdl
RheB Y35A-D65A model	not available	4O25-B	RheB Y35A-D65A-mdl

[a]Two models were generated from the crystal structures of the wild-type and Y35A mutant of RheB GTPase, and two computer-designed mutant models of Y35A and Y35A-D65A were made on the crystal structure of RheB GTPase WT.

Table 2. Production Runs for each System Used in the MD Simulation[a]

model	MD simulation (ns)
WT	4 × 100
Y35A-xtal	4 × 100
Y35A-mdl	4 × 100
Y35A-D65A-mdl	4 × 100

[a]Four independent 100 ns trajectories were run for each of the system, which is represented as 4 × 100 ns.

until the system converged with Fmax no greater than 1000 kJ mol^{-1} nm^{-1}. Equilibration was performed for 600 ps under NVT and for 1200 ps under NPT ensemble while coupling proteins, GTP, ions, and water separately. The temperature was coupled to a V-rescale thermostat with a constant temperature of 300 K while the pressure was maintained at 1 bar using a Berendsen thermostat. The coupling constants for the temperature and pressure to the bath were 0.1 and 1 ps, respectively. The electrostatic interactions were evaluated using the particle mesh Ewald method.[40] A 2 fs integration time step was used for the production run of each simulation. Four independent trajectories of 100 ns each for the WT, Y35A-xtal, Y35A-mdl, and Y35A-D65A-mdl proteins were then performed upon the equilibrated systems using leap-frog algorithm.

Analysis of Trajectories. Analysis was performed on 8000 conformations generated over four MD runs of 100 ns simulation time for each protein. GROMACS tools were used to calculate the root-mean-square deviation, resultant root-mean-square fluctuation (RMSF) of Cα atoms, principal component analysis (PCA) of backbone Cα atoms, and surface area accessibility analysis (SASA) of Cα atoms of proteins and GTP ligand. UCSF Chimera software tool was used for the visualization and calculation of distances between the atoms. Hydrogen bond interactions, timeline analysis of the secondary structure (Timeline plugin), and porcupine plots of the systems were calculated using the visual MD software tool.[41]

Water Residence Time Measurement. The starting structure of the production run in each system was overlaid with the crystal structures of H-Ras (PDB ID 5P21), RheB GTPase WT (PDB ID 4O25 B), and RheB GTPase Y35A (PDB ID 3SEA B). The water molecule in the starting structure of the production run occupying a position similar to the crystallographic equatorial water molecule was designated as the equatorial water molecule for each system. Distance between the oxygen atom of equatorial water and the γ-phosphate of GTP was measured for the entire duration of the simulation time. The time the equatorial water molecule resides at below 4 Å distance from the γ-phosphate of GTP was calculated and reported as residence times.

RESULTS

MD of the Atypical Conformation at the Switch-II Region of the Active Site Correlates with the Slow Intrinsic GTP Hydrolysis Rates of RheB. The switch-II region in the active GTP state of most of the small GTPases has a conserved DxxG motif (57DxxG60 in H-Ras), which stretches into a folded α-helical structure designated as α2 helix (Figures 1B and 2A). The conformation of the analogous region differed in RheB (Figure 1B). The GTP-bound RheB crystal structure (PDB ID 4O25) has two molecules in the asymmetric unit (A and B chains).[36] The conformation of α2 helix differs between the two structures (A and B) in the asymmetric unit of RheB, with the latter being similar to the previously solved structure of RheB with GppNHp (PDB ID 1XTR) (Figure 2A). Although slightly distorted, the structure B of PDB ID 4O25 (WT) still preserves the octahedral conformation of the essential cofactor Mg^{2+} similar to other GTP-bound small GTPases (Figure 2). In the structure A of

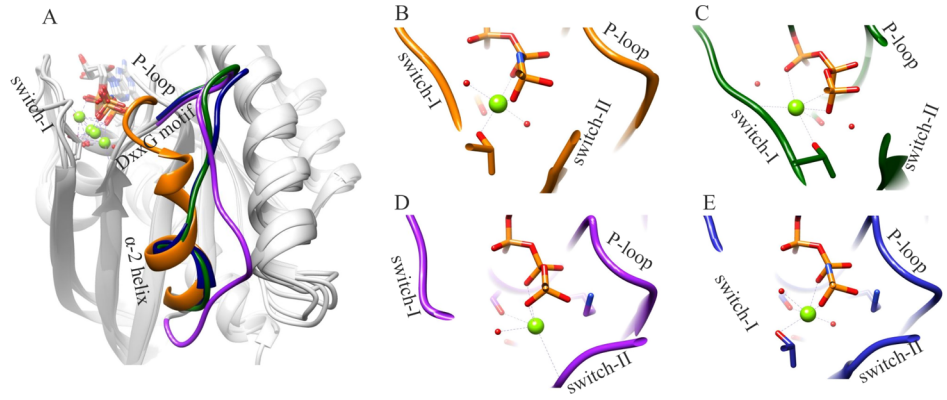

Figure 2. Representation of α2 helix and Mg^{2+} co-ordination in the crystal structures of GTPases. (A) Overlay of crystal structures of H-Ras-GppNHp (PDB ID 5P21) (orange), RheB-GTP (PDB ID 4O25 A) (purple), RheB-GTP (PDB ID 4O25 B) (dark green), and RheB-GppNHp (PDB ID 1XTR) (dark blue). (B) Mg^{2+} co-ordination in H-Ras-GppNHp (PDB ID 5P21). (C) Mg^{2+} co-ordination in RheB-GTP (PDB ID 4O25 B). (D) Mg^{2+} co-ordination in RheB-GTP (PDB ID 4O25 A). (E) Mg^{2+} co-ordination in RheB-GppNHp (PDB ID 1XTR). (Mg^{2+}—light green sphere and water—red sphere).

DOI: 10.1021/acsomega.7b01025
ACS Omega 2017, 2, 6691−6702

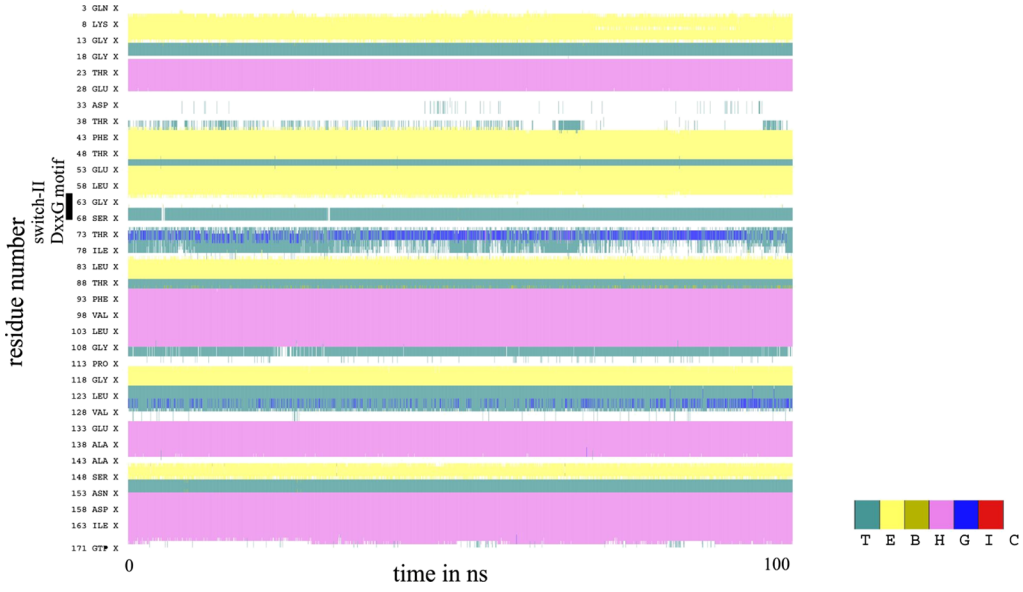

Figure 3. Secondary structure timeline analysis of a single trajectory of the WT. Graphic representation symbol "T" is hydrogen-bonded turn, "E" is the extended parallel or antiparallel β-sheet, "B" is the single pair β-bridge, "H, G, and I" represents the 4-, 3-, and 5-turn helix, respectively, and "C" is the coil.

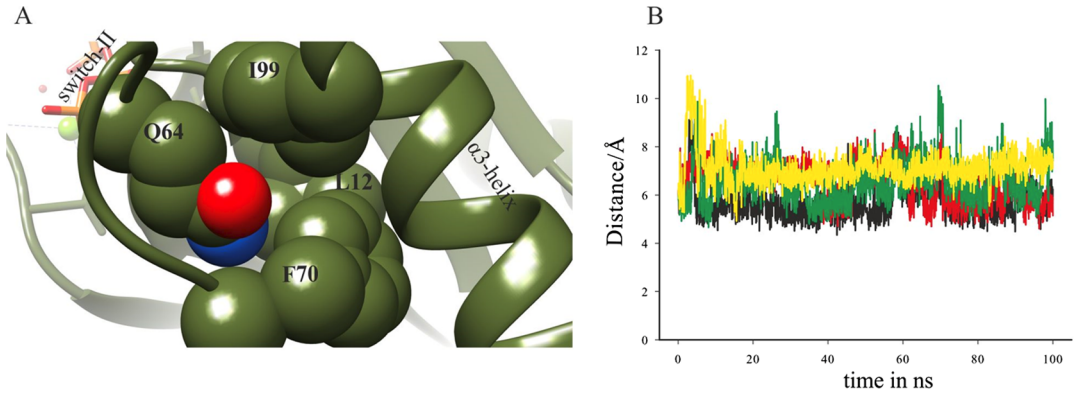

Figure 4. Atypical conformation of Q64 in RheB GTPase. (A) Q64 locked in the hydrophobic groove formed by L12, I99, and F70 (Mg^{2+}—light green sphere and water—red sphere). (B) Distance between side chain amide carbon of Q64 and backbone Cα atom of I99 as a function of time in four trajectories of 100 ns each of the WT (black, red, green, and yellow).

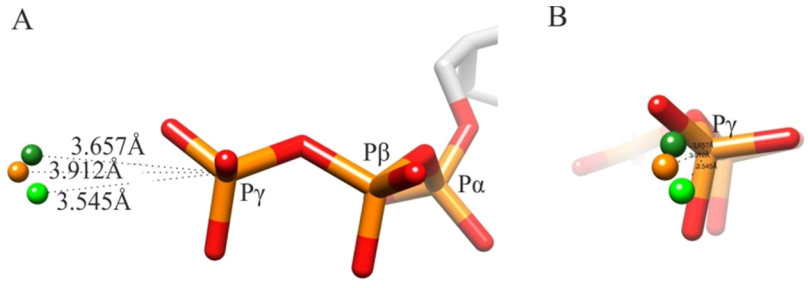

Figure 5. Representation of equitorial water and their distance from γ-phosphate. (A) Longitudinal. (B) Equatorial. (Orange—water in the H-Ras crystal structure (PDB ID 5P21), dark green—water in the RheB crystal structure (PDB ID 4O25 B), and light green—water in WT during the start of the production run).

PDB ID 4O25 however, the Mg^{2+} co-ordination is incomplete with only one water molecule (Figure 2D). Hence, we proceeded with the B structure of PDB ID 4O25 (WT) for our MD simulation studies. Simulations of four independent trajectories of 100 ns each were performed on the WT RheB. We observed that the extended loop conformation with short 3−10 helices persisted over four independent simulations of 100 ns each of the WT (Figures 3 and S2). The immediate downstream neighbor of glycine from the 57DTAG60 (H-Ras) motif in the switch-II region is a conserved glutamine (Q61), which is traditionally recognized as a prerequisite to align the catalytic water molecule for efficient GTP hydrolysis (Figure 1B). The equivalent Q64 in RheB adopts an alternate conformation with its side chain away from the active site

DOI: 10.1021/acsomega.7b01025
ACS Omega 2017, 2, 6691−6702

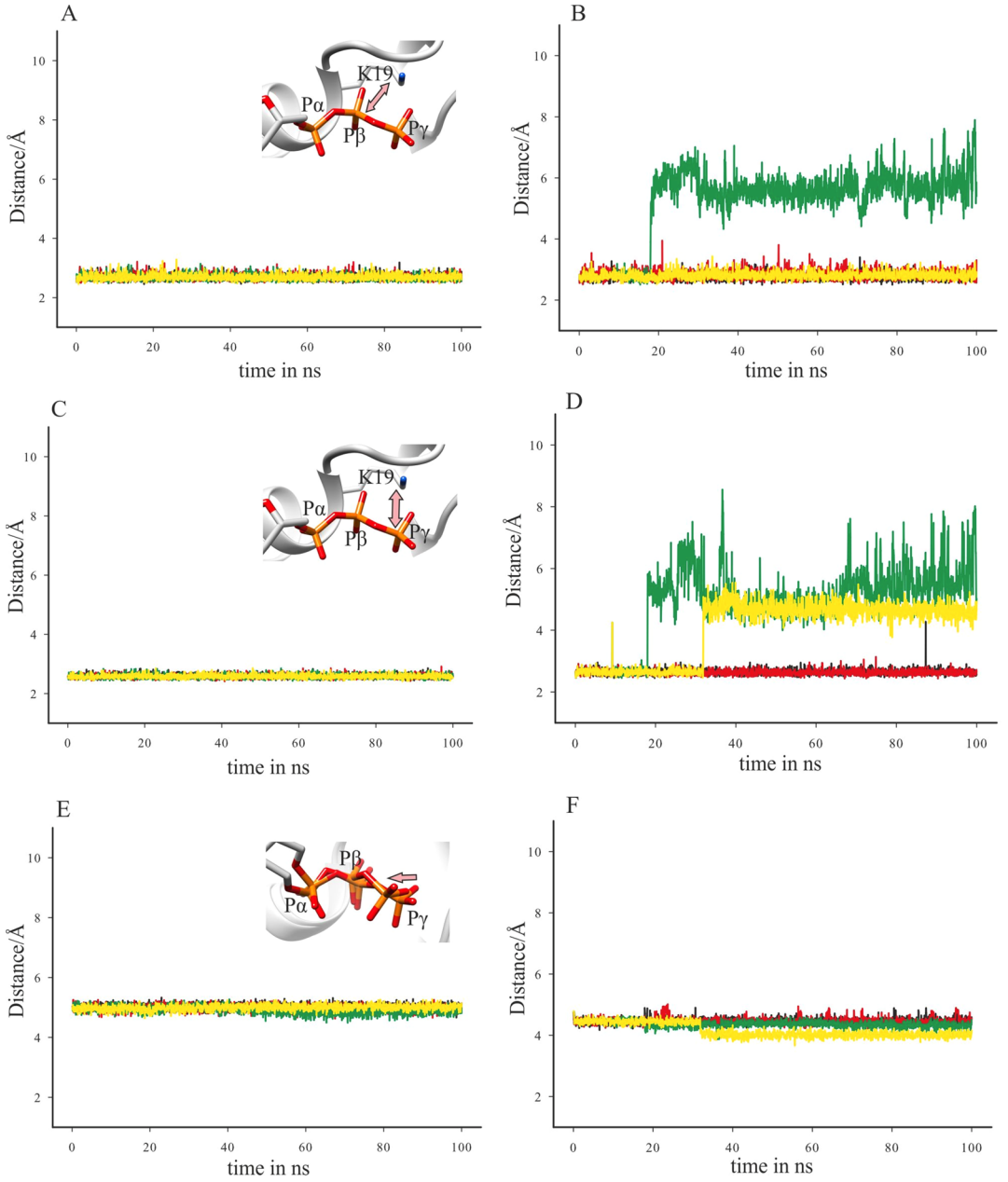

Figure 6. Dynamics of conserved interactions of the guanine nucleotide phosphates and the P loop. (A) Overlay of the distance between β-phosphate atom of GTP and side chain amine nitrogen of K19 (P loop) as a function of time in WT. (B) Overlay of the distance between β-phosphate atom of GTP and side chain amine nitrogen of K19 (P loop) as a function of time in Y35A-xtal. (C) Overlay of the distance between γ-phosphate atom of GTP and side chain amine nitrogen of K19 (P loop) as a function of time in WT. (D) Overlay of the distance between γ-phosphate atom of GTP and side chain amine nitrogen of K19 (P loop) as a function of time in Y35A-xtal. (E) Overlay of the distance between the Pα and Pγ atoms of GTP as a function of time in WT. (F) Overlay of the distance between the Pα and Pγ atoms of GTP as a function of time in Y35A-xtal (black, red, green, and yellow represent four independent trajectories of 100 ns each).

(Figure 1B). Previous structural studies had assumed that this might be because of the bulky side chain of the proximal R15 residue from the P loop[35] (Figure 1B). The analogous residue in H-Ras is G12, which is suggested to confer dynamic flexibility to the proximal catalytic glutamine residue of the switch-II region because of the absence of side chain[32,36] (Figure 1). Interestingly, in our study, the side chain of the conserved Q64 remains locked in the hydrophobic groove formed by L12, P70 and I99, maintaining the orientation of the Q64 side chain away from the active site for the entire simulation period (Figures 3, 4, and S2).

The crystal structure of RheB shows a water molecule near the γ-phosphate of GTP, analogous to the catalytic equatorial water of H-Ras[11,32] (Figure 5). Although crystallographic water molecules were removed prior to the system preparation, a water molecule at a similar position was observed during the start of the simulation of RheB wild type (Figure 5). However, this water molecule was exchanged within 1 ns timescale with the bulk solvent, suggesting the absence of stabilizing interactions in the vicinity (Figure S3). Therefore, we assume that the stable atypical conformation of the conserved Q64 in the switch-II region would not provide a favorable local electrostatic environment for the GTP catalysis by an equatorial

DOI: 10.1021/acsomega.7b01025
ACS Omega 2017, 2, 6691−6702

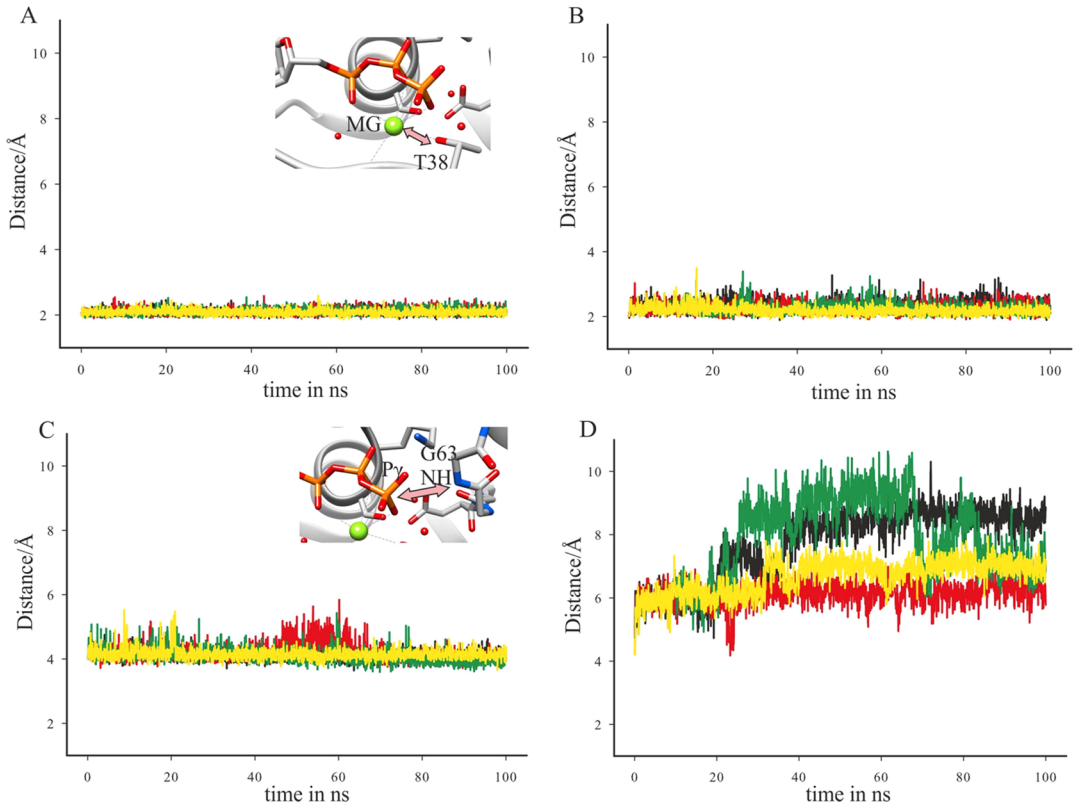

Figure 7. Dynamics of conserved interactions of the switch regions near the active site. (A) Overlay of the distance between Mg^{2+} and oxygen atom of side chain hydroxyl of T38 (switch-I) as a function of time in WT. (B) Overlay of the distance between Mg^{2+} and oxygen atom of side chain hydroxyl of T38 (switch-I) as a function of time in Y35A-xtal. (C) Overlay of the distance between Pγ atom of GTP and backbone nitrogen of atom of G63 (switch-II) as a function of time in WT. (D) Overlay of the distance between Pγ atom of GTP and backbone nitrogen of atom of G63 (switch-II) as a function of time in Y35A-xtal (black, red, green, and yellow represent four independent trajectories of 100 ns each).

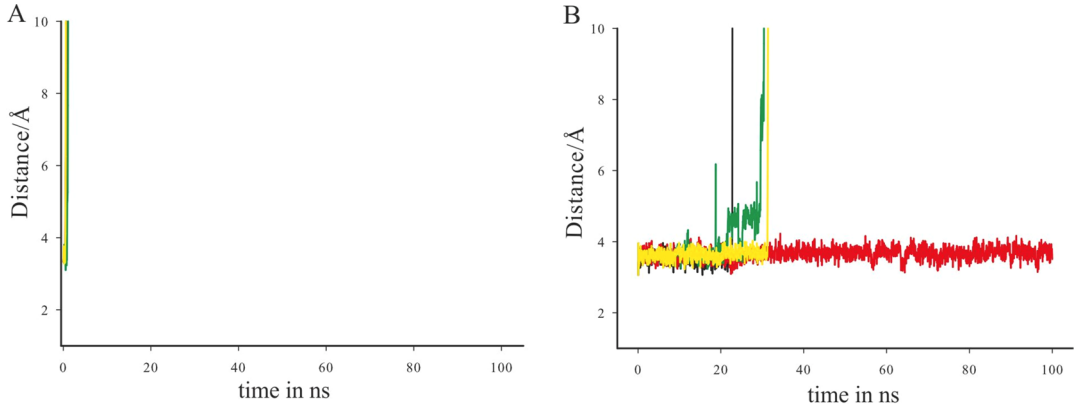

Figure 8. Residence time of equitorial water. (A) Distance between the Pγ atom of GTP and oxygen of equitorial water as a function of time in WT. (B) Distance between the Pγ atom of GTP and oxygen of equitorial water as a function of time in Y35A-xtal (black, red, green, and yellow represent four independent trajectories of 100 ns each).

water molecule. Added to this, the low residence time of equatorial water (<1 ns) will further diminish the chances for efficient GTP hydrolysis by RheB.

Y35A Mutation Affects the Stability of Conserved Interactions and Water Dynamics at the Active Site. Previous studies have shown that the Y35A mutation in RheB GTPase accelerates its intrinsic GTP catalysis rates comparable to H-Ras.[36] The crystal structure of Y35A mutant (PDB ID 3SEA) indicates two conformations in the crystal lattice, each one bound to GDP and GppNHp[36] (also discussed in Methods section). The GppNHp-bound structure of RheB Y35A mutant (Y35A-xtal) displayed only minor conformational variations such as increased solvent exposure of the nucleotide binding pocket and reduced distance between the equatorial water molecule and the side chain hydroxyl of T38, compared to the wild type[36] (Figure S1B). The increased rate of GTP hydrolysis of Y35A mutant was attributed to favorable thermodynamics. Overall, the activation free energy of hydrolysis was decreased in Y35A mutant. The bulky electron-rich phenol side chain of Y35 was assumed to destabilize the transition state.[36] We further wanted to investigate the differences in structural

DOI: 10.1021/acsomega.7b01025
ACS Omega 2017, 2, 6691−6702

dynamics associated with the fast hydrolyzing Y35A mutant of RheB.

We found several differences in the dynamics and stability of the GTP nucleotide in our simulations of Y35A-xtal. The K19 of P loop is highly conserved among small GTPases and is responsible for neutralizing the negative charge of GTP by interacting with the β- and γ-phosphates of the GTP nucleotide. Compared to the WT, Y35A-xtal showed notable fluctuation in the interaction of β- and γ-phosphates with the K19 of the P loop (Figure 6A–D). Previous studies have discussed the conformations adopted by α-, β-, and γ-phosphates of GTP when bound to H-Ras.[19] Here, we observed that the γ-phosphate has variable dynamics in the simulations of Y35A-xtal compared to WT. We further quantified this difference by measuring the distance between α- and γ-phosphate atoms of GTP (Figure 6E,F). In the switch-I region, elevated dynamics were observed in the interaction of the conserved T38 and Mg^{2+} ion (Figure 7A,B). In Y35A-xtal, at switch-II region, the hydrogen bond between backbone amide nitrogen (NH) of glycine and oxygen of the γ-phosphate of GTP fluctuates in comparison with the stable hydrogen bond observed in WT (Figure 7C,D). These observations suggest that the Y35A mutation destabilizes the conserved interactions of active site residues with the phosphates of GTP nucleotide and Mg^{2+}. Interestingly, the equatorial water remains for longer periods of time in all trajectories compared to the WT (Figures 5 and 8). Previous experimental study has shown that the Y35A mutation in RheB GTPase would improve its slow intrinsic GTP hydrolysis rates similar to that of H-Ras.[36] We propose that the destabilization of γ-phosphate of GTP in the active site of Y35A-xtal might favor its efficient removal. Similarly, the greater residence time of the equatorial water would improve the chances for the equatorial water to catalyze GTP hydrolysis. Taken together, our results show the variable conformational dynamics observed in the GTP binding site of Y35A-xtal which may provide the basis for the reported accelerated rates of GTP hydrolysis in the Y35A mutant of RheB GTPase.[36,42]

RMSF Plots Reveal Distinctive Cα Fluctuations in the 3–10 Helix and Switch-I and Switch-II Regions of the Wild Type and Its Y35A Mutant. We compared the flexibility of each amino acid residue in the WT and Y35A-xtal by calculating the RMSF of each α-carbon over four 100 ns simulations of both the proteins. The RMSF profiles are similar between the two proteins except at the regions corresponding to the short 3–10 helix downstream of switch-II and the switch-I regions (Figure 9A). As anticipated, the switch regions displayed variation in the fluctuation of the backbone Cα atoms because of the lack of stabilizing interaction between Y35 and γ-phosphate (Figure 9A). We observed that the high fluctuation in the Cα atoms in the switch-I region of the WT is because of the substantial conformational flipping in the residues corresponding to D33, S34, and Y35 (Figure 9A). The switch-II region displayed notable fluctuation corresponding to the G63 of ^{60}DxxG^{63} motif, which as mentioned previously is involved in the backbone amide and phosphate oxygen interaction (Figure 7D). At the 3–10 helix, the WT showed a significant variation in the Cα fluctuation compared to its mutant (Figure 9A). A closer look at MD in this region revealed that the E40 of switch-I and Y74 of 3–10 helix are at a potential hydrogen bond interaction distance (Figure 9A). Indeed, occupancy measurements revealed the presence of a hydrogen bond between the two residues (Figure S4). To evaluate the stability of this interaction, we plotted the distance

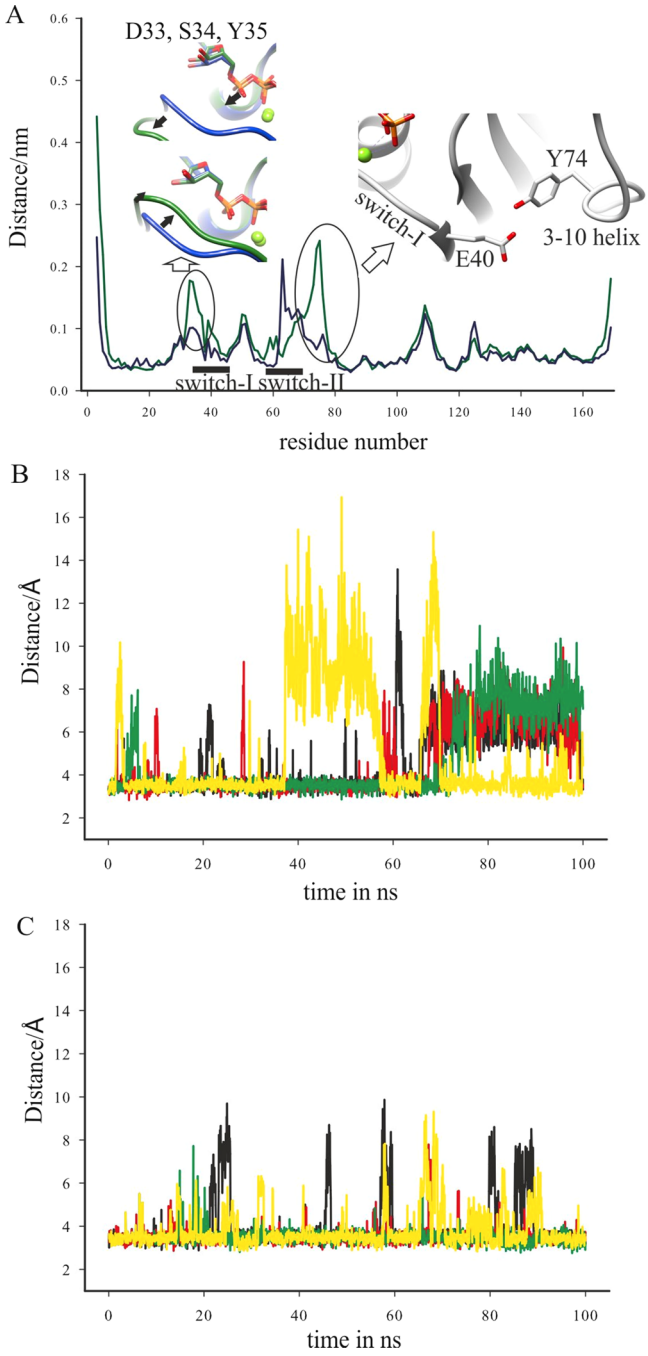

Figure 9. RMSF plot of Cα atoms of WT and Y35-xtal. (A) Overlay of RMSF plots of the WT (dark green) and Y35A-xtal (dark blue) of RheB GTPase. (B) Overlay of the distance between the side chain Cγ atom of E40 and oxygen atom of side chain hydroxyl of Y74 as a function of time in WT (black, red, green, and yellow represent four independent trajectories). (C) Overlay of the distance between the side chain Cγ atom of E40 and oxygen atom of side chain hydroxyl of Y74 as a function of time in Y35A-xtal (black, red, green, and yellow represent four independent trajectories of 100 ns each).

between the side chain Cγ atom of E40 and oxygen atom of side chain hydroxyl of Y74 as a function of time (Figure 9B,C). The measurements were performed for four 100 ns MD trajectories of the WT and Y35A-xtal proteins. The analysis showed a significant fluctuation in the distances between the two atoms in the WT compared to its mutant (Figure 9B,C). The dynamics at the interface of switch-I and switch-II regions

DOI: 10.1021/acsomega.7b01025
ACS Omega 2017, 2, 6691–6702

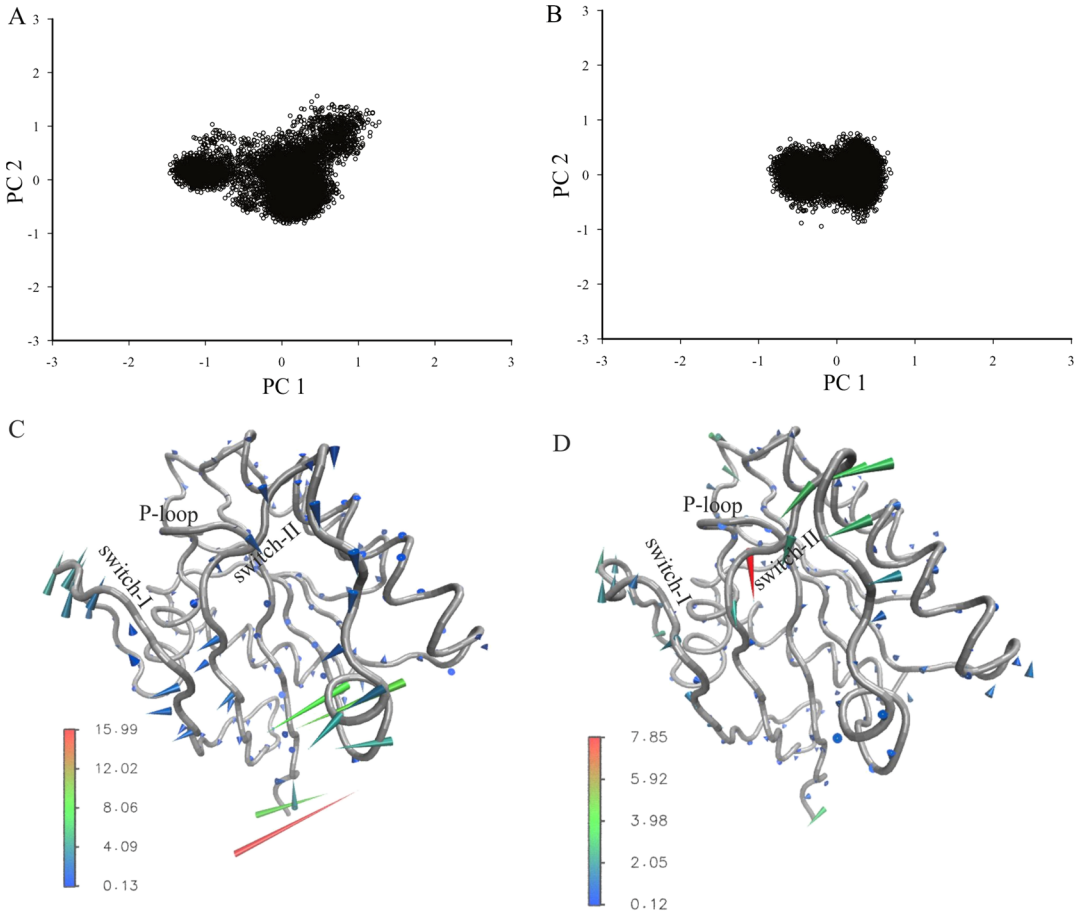

Figure 10. PCA. (A) Projection of MD trajectories on the first two principal components of WT. (B) Projection of MD trajectories on the first two principal components of Y35A-xtal. (C) Porcupine plot showing the significant motions in the WT. (D) Porcupine plot showing the significant motions in Y35A-xtal. Arrows on the protein backbone show the direction and the magnitude of the correlated motion. The red color of the arrows depicts the highest movement followed by green, whereas blue depicts the least movement.

are critical for coordinated transition from closed (GTP) state to open (GDP) state.[43,44] Because this interaction is away from the catalytic site, it indirectly indicates that the highly dynamic 3−10 helix in the WT may interfere with the efficient GTP to GDP conformational transition, accounting for the slow intrinsic GTP hydrolysis rates of RheB GTPase.

PCA Reveals Notable Variation in the Collective Dynamics of the Proteins. PCA is a well-known technique to analyze the functional collective motions from MD simulation trajectories. To probe the effect of mutations on the overall combined motion of RheB, we performed Cα PCA for each system. The projections of PC1 and PC2 for the WT and Y35A-xtal consist of a structural ensemble of two clusters (Figure 10A,B). The scatter plots indicate that there is a difference in the eigenvectors computed from the MD trajectories of both the systems. Further, the WT samples show greater conformational space compared to Y35A-xtal (Figure 10A,B). To visualize the components that contribute mostly to the overall motion, porcupine plots for Cα atoms were made using the two extreme structures generated from the eigenvectors of both the systems (Figure 10C,D). Interestingly, the dominant motions observed in both the systems corroborate with their aforementioned dynamics (Figures 7C,D, 9, and 10C,D). The greater conformational sampling in the WT is contributed by the large motions in the N-terminal and 3−10 helix downstream of the switch-II region (Figure 10C). The 3−10 helix region also harbors the E40-Y74 hydrogen bond interaction which is not stable in the WT compared to Y35A-xtal (Figure 9). Similarly, the motions in the switch-II region of Y35A-xtal concur with its previously quantified variable dynamics between the backbone amide (NH) of G63 and γ-phosphate of GTP (Figures 10B and 7D). Together, these results show that the increase in hydrolysis rates of the Y35A mutant is accompanied by an overall change in its molecular motions and its associated conformational dynamics.

MD Simulations of the Y35A-mdl and Y35A-D65A-mdl Systems Provide Additional Insights into the Reduced GTP Hydrolysis Rate of Y35A-D65A Mutant. Previous studies have shown that the Y35A-D65A double mutation reduces the enhanced intrinsic GTP hydrolysis rates of the Y35A mutant by at least 60%.[36] The contrasting dynamics observed between the WT and Y35A-xtal provided the impetus to decipher the molecular motions of the Y35A-D65A double mutant. Because no crystal structure is available for the Y35A-D65A double mutant, we used the in silico-generated double mutation on WT as a starting model for the MD simulation (Table 1). Simultaneously, we also generated Y35A in silico single mutant (Table 1) to compare, correlate, and understand the conformational dynamics of in silico-generated Y35A-D65A double mutant (Table 1). Both Y35A-mdl and Y35A-D65A-mdl systems were simulated for four 100

DOI: 10.1021/acsomega.7b01025
ACS Omega 2017, 2, 6691−6702

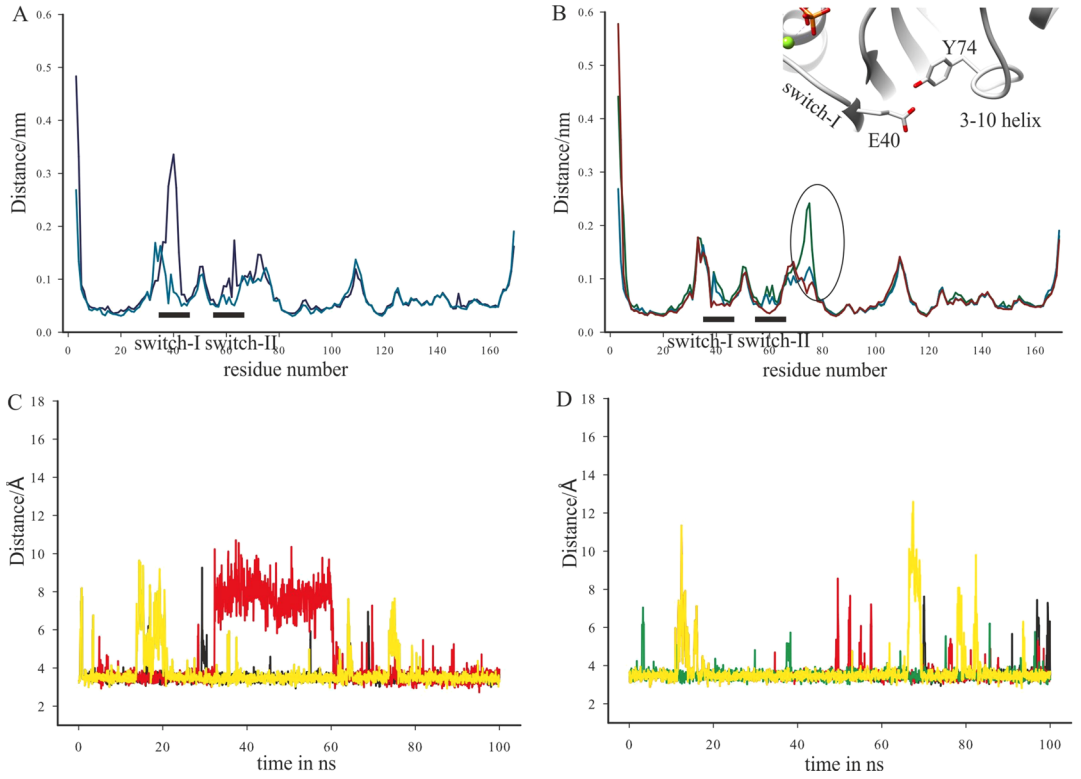

Figure 11. RMSF plot of Cα atoms of WT and Y35A-mdl and Y35A-D65A-mdl mutants. (A) Overlay of RMSF plots of the Y35A-xtal (dark blue)- and Y35A-mdl (dark cyan) mutants. (B) Overlay of RMSF plots of the WT (dark green) and Y35A-mdl (dark cyan) and Y35A-D65A-mdl (dark brown color) mutants of RheB GTPase. (C) Overlay of the distance between the side chain Cγ atom of E40 and oxygen atom of side chain hydroxyl of Y74 as a function of time in Y35A-mdl (black, red, green, and yellow represent four independent trajectories). (D) Overlay of the distance between the side chain Cγ atom of E40 and oxygen atom of side chain hydroxyl of Y74 as a function of time in Y35A-D65A-mdl (black, red, green, and yellow represent four independent trajectories of 100 ns each).

ns independent trajectories similar to the WT (Table 2). Y35A-mdl did not show significant changes in the dynamics of the interactions of the conserved residues of switch-I and switch-II with GTP nucleotide and Mg^{2+} as previously described for Y35A-xtal, suggesting that the simulations would need to be run for a sufficiently long time for the system to reach the energy minima of Y35A-xtal (Figure 11A). Despite this, the RMSF plots of Y35A-mdl and Y35A-D65A-mdl showed similar consistent interaction between E40 and Y74 (Figures 11B–D and S4). In addition, the double mutant displayed reduced Cα fluctuations in the switch regions (Figure 11B). The PCA porcupine plots indicate that Y35A-D65A-mdl has dominant motions at the N-terminal similar to the WT (Figures 10C and S5D). However, the rest of Y35A-D65A-mdl including the switch regions displayed restricted motions compared to the WT (Figures 10C and S5D). Previous experimental studies have shown that the electronegative D65 residue is required for aligning the catalytic water molecule similar to the conventional glutamine in H-Ras.[36] Therefore, our results show that the additional D65A mutation would possibly constrain the dynamics of switch regions accounting for the reduction in the hydrolysis rates observed for the double mutant. Unlike the WT, the residence time of equatorial water is also sufficiently longer in the simulation of Y35A-xtal, suggesting efficient GTP hydrolysis (Figure 8). Despite the very low residence time of analogous water molecule in the simulation of computer-generated mutants, the water molecule in Y35A-mdl stays at least double the amount of time as the WT before being exchanged with the bulk solvent (Figure S3). These observations suggest a similar trend for the simulation of Y35A-mdl as the crystal structure. In addition, the PCA and RMSF plots of the double mutant show the possible role for the distinct collective motions and reduced switch region dynamics for the reduced rate of GTP hydrolysis (Figures 11B and S5).

DISCUSSION

The mechanism of intrinsic/GAP-mediated GTP hydrolysis in H-Ras GTPase dictates the imperative role for a conserved glutamine (Q61) of switch-II region.[32,45,46] Therefore, until recently, the glutamine to leucine mutants of Ras superfamily GTPases were used as constitutively active proteins for cellular studies.[33,47,48] However, recent studies have detailed the potential disparity between the expected and observed phenotypes of such mutations.[49] For RheB (Ras homology enriched in brain), the analogous conserved glutamine adopts the atypical conformation with its side chain pointed away from the active site (Figure 1B). Accordingly, its leucine mutation does not affect the function of the RheB GTPase.[35,36] The atypical conformation of the conserved glutamine was reasoned to be a consequence of proximal bulky side chain of R15 from P loop (Figure 1B). However, the arginine to glycine mutation does not affect the intrinsic hydrolysis rates of RheB, suggesting that the conformation of glutamine side chain remains unaltered even after the mutation.[36] Our results corroborate this and show that the side chain of the conserved Q64 remains packed in a crowded hydrophobic environment remote from the influence of R15 side chain (Figure 4).

DOI: 10.1021/acsomega.7b01025
ACS Omega 2017, 2, 6691−6702

Y35 of the switch-I region is highly conserved among Ras and Rho family GTPases compared to the Rab GTPases. However, the analogous Y-to-A mutation on slow, intrinsically hydrolyzing Rab6 and Rab7 GTPases is shown to increase their rates by several fold.[45,50] Although the exact role of tyrosine still remains elusive, studies assume it to influence the GTP hydrolysis process by blocking the access to bulk water.[50] Similarly, the analogous Y35A mutation of RheB GTPase is shown to accelerate its GTP hydrolysis activity.[36] Our SASA analysis of Cα atoms of protein and GTP ligand revealed only minor variations between the WT and Y35A-xtal (Figure S6). Interestingly, we observed noticeable variations in the stability of several conserved interactions of Y35A-xtal with GTP and Mg^{2+} (Figures 6 and 7). Moreover, the mutation also impairs the traditional octahedral geometry of Mg^{2+} ion[20,30] (Figure 2A). In addition, the mutation also stabilizes the positioning of equatorial water with interactions from oxygen atoms of γ-phosphate and backbone oxygen of T38 (Figures 5 and 8 and S7). The dynamic flexibility of γ-phosphate and accessibility of stable equatorial water concur with the previously established elevated rates of GTP hydrolysis in RheB Y35A mutant.[36,42]

The Cα RMSF plot of Y35A-mdl differed from Y35A-xtal only at the catalytic switch regions (Figure 11A). Accordingly, the variable dynamics previously observed at the active site of Y35A-xtal simulations were not seen in the simulations of Y35A-mdl (Figures 6 and 7). Unlike Y35A-xtal, the starting model for Y35A-mdl would have residue network organization identical to that in the WT. We assume that the system may need to be energy minimized and run for a sufficiently long time to reach the energy minima of Y35A-xtal. In agreement, the PCA overlay shows the ensemble of two clusters at similar positions but varied densities (Figure S5A). However, Y35A-mdl showed a trend in dynamics at the 3−10 helix similar to that in Y35A-xtal (Figure 11B,C). These observed variations were taken into account while analyzing the simulations of Y35A-D65A-mdl. The RMSF plots of Y35A-D65A-mdl showed restricted dynamics at the catalytic switch regions. The motions in the porcupine plots also indicate restricted motions in the switch regions of Y35A-D65A-mdl compared to the other systems in the study (Figures 10, S5). Similarly, the residence time for equatorial water was unusually short as compared to Y35A-mdl (Figures 11B and S3). On the basis of these observations, we speculate an additional role for the D65 residue in conferring dynamic flexibility to the switch regions of RheB, in addition to its previously described role as a potential water-aligning residue.[36]

Recent studies have identified several point mutations at distinct positions of RheB GTPase that are associated with several cancers.[34,51] The E40 of switch-I is involved in contrasting fluctuations with its interaction of Y74 of 3−10 helix between the WT and Y35A-xtal/Y35A-mdl (Figures 9 and 11). Interestingly, E40K is one of the several mutants identified in the renal cancers.[52] Similarly, Y35N is the most recurring oncogenic point mutation observed in RheB.[51] Although the exact structural basis is yet to be identified, Y35N mutation was shown to act as a hyperactive GTPase inside the cell.[51] Our work on Y35A mutation provides preliminary assessment of the possible destabilization effects on the γ-phosphate of GTP nucleotide. However, separate studies need to be conducted to arrive at a comprehensive understanding of the functioning of these mutants. Taken together, our findings provide fresh insights into the molecular basis for the noncanonical mode of GTP hydrolysis in RheB. Further, it provides the mechanistic evidence for the differential modulation of GTP catalysis by RheB mutants Y35A and Y35A-D65A.

■ ASSOCIATED CONTENT

Supporting Information

The Supporting Information is available free of charge on the ACS Publications website at DOI: 10.1021/acsomega.7b01025.

Supporting information available with additional figures (PDF)

■ AUTHOR INFORMATION

Corresponding Authors

*E-mail: ckotyada@gmail.com (C.K.).
*E-mail: singh@iisc.ac.in (M.S.).

ORCID

Mahavir Singh: 0000-0003-1251-8248

Author Contributions

Conceived and designed experiments: C.K.; analyzed data: C.K., M.S., A.M., and A.S.; wrote paper: C.K. and M.S.; and contributed to the writing of the paper and discussions of the analysis of the simulations: A.M. and A.S.

Funding

This work is supported by the Indian Institute of Science (M.S.), the IISc-DBT Partnership Program (M.S.), and the Department of Biotechnology (M.S. and C.K.).

Notes

The authors declare no competing financial interest.

■ ACKNOWLEDGMENTS

We sincerely acknowledge Dr. Rajesh Murarka (Assistant Professor, IISER Bhopal, India) for sharing with us the Charmm27 force field parameters for GTP.

■ REFERENCES

(1) Wittinghofer, A.; Waldmann, H. Ras—A molecular switch involved in tumor formation. *Angew. Chem., Int. Ed.* **2000**, *39*, 4192−4214.

(2) White, M. A.; Nicolette, C.; Minden, A.; Polverino, A.; Van Aelst, L.; Karin, M.; Wigler, M. H. Multiple Ras Functions Can Contribute to Mammalian Cell Transformation. *Cell* **1995**, *80*, 533−541.

(3) Barr, F.; Lambright, D. G. Rab GEFs and GAPs. *Curr. Opin. Cell Biol.* **2010**, *22*, 461−470.

(4) Hein, C.; Wittinghofer, A.; Dötsch, V. How to switch a master switch. *eLife* **2013**, *2*, e01159.

(5) Buhrman, G.; Kumar, V. S. S.; Cirit, M.; Haugh, J. M.; Mattos, C. Allosteric modulation of Ras-GTP is linked to signal transduction through RAF kinase. *J. Biol. Chem.* **2011**, *286*, 3323−3331.

(6) Simpson, J. C.; Griffiths, G.; Wessling-Resnick, M.; Fransen, J. A. M.; Bennett, H.; Jones, A. T. A role for the small GTPase Rab21 in the early endocytic pathway. *J. Cell Sci.* **2004**, *117*, 6297−6311.

(7) Geyer, M.; Herrmann, C.; Wohlgemuth, S.; Wittinghofer, A.; Kalbitzer, H. R. Structure of the Ras-binding domain of RalGEF and implications for Ras binding and signalling. *Nat. Struct. Biol.* **1997**, *4*, 694−699.

(8) Vetter, I. R.; Nowak, C.; Nishimoto, T.; Kuhlmann, J.; Wittinghofer, A. Structure of a Ran-binding domain complexed with Ran bound to a GTP analogue: implications for nuclear transport. *Nature* **1999**, *398*, 39−46.

(9) Pai, E. F.; Kabsch, W.; Krengel, U.; Holmes, K. C.; John, J.; Wittinghofer, A. Structure of the guanine-nucleotide-binding domain of the Ha-ras oncogene product p21 in the triphosphate conformation. *Nature* **1989**, *341*, 209−214.

DOI: 10.1021/acsomega.7b01025
ACS Omega 2017, 2, 6691−6702

(10) Wittinghofer, A.; Vetter, I. R. Structure-Function Relationships of the G Domain, a Canonical Switch Motif. *Annu. Rev. Biochem.* **2011**, *80*, 943−971.
(11) Buhrman, G.; Holzapfel, G.; Fetics, S.; Mattos, C. Allosteric modulation of Ras positions Q61 for a direct role in catalysis. *Proc. Natl. Acad. Sci. U.S.A.* **2010**, *107*, 4931−4936.
(12) Prior, I. A.; Lewis, P. D.; Mattos, C. A comprehensive survey of Ras mutations in cancer. *Cancer Res.* **2012**, *72*, 2457−2467.
(13) Marcus, K.; Mattos, C. Direct Attack on RAS: Intramolecular Communication and Mutation-Specific Effects. *Clin. Cancer Res.* **2015**, *21*, 1810−1818.
(14) Nussinov, R.; Tsai, C.-J.; Mattos, C. "Pathway drug cocktail": targeting Ras signaling based on structural pathways. *Trends Mol. Med.* **2013**, *19*, 695−704.
(15) Xia, F.; Rudack, T.; Cui, Q.; Kötting, C.; Gerwert, K. Detailed structure of the H2PO4(-)-guanosine diphosphate intermediate in Ras-GAP decoded from FTIR experiments by biomolecular simulations. *J. Am. Chem. Soc.* **2012**, *134*, 20041−20044.
(16) Kotting, C.; Kallenbach, A.; Suveyzdis, Y.; Wittinghofer, A.; Gerwert, K. The GAP arginine finger movement into the catalytic site of Ras increases the activation entropy. *Proc. Natl. Acad. Sci. U.S.A.* **2008**, *105*, 6260−6265.
(17) Chakrabarti, P. P.; Daumke, O.; Suveyzdis, Y.; Kötting, C.; Gerwert, K.; Wittinghofer, A. Insight into catalysis of a unique GTPase reaction by a combined biochemical and FTIR approach. *J. Mol. Biol.* **2007**, *367*, 983−995.
(18) Kotting, C.; Blessenohl, M.; Suveyzdis, Y.; Goody, R. S.; Wittinghofer, A.; Gerwert, K. A phosphoryl transfer intermediate in the GTPase reaction of Ras in complex with its GTPase-activating protein. *Proc. Natl. Acad. Sci. U.S.A.* **2006**, *103*, 13911−13916.
(19) Rudack, T.; Xia, F.; Schlitter, J.; Kotting, C.; Gerwert, K. Ras and GTPase-activating protein (GAP) drive GTP into a precatalytic state as revealed by combining FTIR and biomolecular simulations. *Proc. Natl. Acad. Sci. U.S.A.* **2012**, *109*, 15295−15300.
(20) Rudack, T.; Xia, F.; Schlitter, J.; Kötting, C.; Gerwert, K. The Role of Magnesium for Geometry and Charge in GTP Hydrolysis, Revealed by Quantum Mechanics/Molecular Mechanics Simulations. *Biophys. J.* **2012**, *103*, 293−302.
(21) Xia, F.; Rudack, T.; Kötting, C.; Schlitter, J.; Gerwert, K. The specific vibrational modes of GTP in solution and bound to Ras: a detailed theoretical analysis by QM/MM simulations. *Phys. Chem. Chem. Phys.* **2011**, *13*, 21451−21460.
(22) Cepus, V.; Scheidig, A. J.; Goody, R. S.; Gerwert, K. Time-resolved FTIR studies of the GTPase reaction of H-ras p21 reveal a key role for the β-phosphate. *Biochemistry* **1998**, *37*, 10263−10271.
(23) Hall, B. E.; Bar-Sagi, D.; Nassar, N. The structural basis for the transition from Ras-GTP to Ras-GDP. *Proc. Natl. Acad. Sci. U.S.A.* **2002**, *99*, 12138−12142.
(24) Ford, B.; Hornak, V.; Kleinman, H.; Nassar, N. Structure of a transient intermediate for GTP hydrolysis by Ras. *Structure* **2006**, *14*, 427−436.
(25) Nassar, N.; Singh, K.; Garcia-Diaz, M. Structure of the Dominant Negative S17N Mutant of Ras. *Biochemistry* **2010**, *49*, 1970−1974.
(26) Ford, B.; Skowronek, K.; Boykevisch, S.; Bar-Sagi, D.; Nassar, N. Structure of the G60A mutant of Ras. *J. Biol. Chem.* **2005**, *280*, 25697−25705.
(27) Brondyk, W. H.; McKiernan, C. J.; Burstein, E. S.; Macara, I. G. Mutants of Rab3A analogous to oncogenic Ras mutants. Sensitivity to Rab3A-GTPase activating protein and Rab3A-guanine nucleotide releasing factor. *J. Biol. Chem.* **1993**, *268*, 9410−9415.
(28) Dumas, J. J.; Zhu, Z.; Connolly, J. L.; Lambright, D. G. Structural basis of activation and GTP hydrolysis in Rab proteins. *Structure* **1999**, *7*, 413−423.
(29) Spoerner, M.; Herrmann, C.; Vetter, I. R.; Kalbitzer, H. R.; Wittinghofer, A. Dynamic properties of the Ras switch I region and its importance for binding to effectors. *Proc. Natl. Acad. Sci. U.S.A.* **2001**, *98*, 4944−4949.
(30) John, J.; Rensland, H.; Schlichting, I.; Vetter, I.; Borasio, G. D.; Goody, R. S.; Wittinghofer, A. Kinetic and Structural-Analysis of the Mg2+-Binding Site of the Guanine Nucleotide-Binding Protein P21(H-Ras). *J. Biol. Chem.* **1993**, *268*, 923−929.
(31) Martín-García, F.; Mendieta-Moreno, J. I.; López-Viñas, E.; Gómez-Puertas, P.; Mendieta, J. The Role of Gln61 in HRas GTP hydrolysis: a quantum mechanics/molecular mechanics study. *Biophys. J.* **2012**, *102*, 152−157.
(32) Frech, M.; Darden, T. A.; Pedersen, L. G.; Foley, C. K.; Charifson, P. S.; Anderson, M. W.; Wittinghofer, A. Role of Glutamine-61 in the Hydrolysis of Gtp by P21(H-Ras): an Experimental and Theoretical Study. *Biochemistry* **1994**, *33*, 3237−3244.
(33) Buhrman, G.; Wink, G.; Mattos, C. Transformation efficiency of RasQ61 mutants linked to structural features of the switch regions in the presence of Raf. *Structure* **2007**, *15*, 1618−1629.
(34) Heard, J. J.; Fong, V.; Bathaie, S. Z.; Tamanoi, F. Recent progress in the study of the Rheb family GTPases. *Cell. Signalling* **2014**, *26*, 1950−1957.
(35) Yu, Y.; Li, S.; Xu, X.; Li, Y.; Guan, K.; Arnold, E.; Ding, J. Structural basis for the unique biological function of small GTPase RHEB. *J. Biol. Chem.* **2005**, *280*, 17093−17100.
(36) Mazhab-Jafari, M. T.; Marshall, C. B.; Ishiyama, N.; Ho, J.; Di Palma, V.; Stambolic, V.; Ikura, M. An autoinhibited noncanonical mechanism of GTP hydrolysis by Rheb maintains mTORC1 homeostasis. *Structure* **2012**, *20*, 1528−1539.
(37) Marshall, C. B.; Ho, J.; Buerger, C.; Plevin, M. J.; Li, G.-Y.; Li, Z.; Ikura, M.; Stambolic, V. Characterization of the Intrinsic and TSC2-GAP-Regulated GTPase Activity of Rheb by Real-Time NMR. *Sci. Signaling* **2009**, *2*, ra3.
(38) Pettersen, E. F.; Goddard, T. D.; Huang, C. C.; Couch, G. S.; Greenblatt, D. M.; Meng, E. C.; Ferrin, T. E. UCSF Chimera−a visualization system for exploratory research and analysis. *J. Comput. Chem.* **2004**, *25*, 1605−1612.
(39) Jorgensen, W. L.; Chandrasekhar, J.; Madura, J. D.; Impey, R. W.; Klein, M. L. Comparison of Simple Potential Functions for Simulating Liquid Water. *J. Chem. Phys.* **1983**, *79*, 926−935.
(40) Darden, T.; York, D.; Pedersen, L. Particle Mesh Ewald—an N Log(N) Method for Ewald Sums in Large Systems. *J. Chem. Phys.* **1993**, *98*, 10089−10092.
(41) Humphrey, W.; Dalke, A.; Schulten, K. VMD: Visual molecular dynamics. *J. Mol. Graphics Modell.* **1996**, 33−38.
(42) Marshall, C. B.; Ho, J.; Buerger, C.; Plevin, M. J.; Li, G.-Y.; Li, Z.; Ikura, M.; Stambolic, V. Characterization of the Intrinsic and TSC2-GAP-Regulated GTPase Activity of Rheb by Real-Time NMR. *Sci. Signaling* **2009**, *2*, ra3.
(43) Grant, B. J.; Gorfe, A. A.; McCammon, J. A. Ras Conformational Switching: Simulating Nucleotide-Dependent Conformational Transitions with Accelerated Molecular Dynamics. *PLoS Comput. Biol.* **2009**, *5*, No. e1000325.
(44) Kobayashi, C.; Saito, S. Relation between the Conformational Heterogeneity and Reaction Cycle of Ras Molecular Simulation of Ras. *Biophys. J.* **2010**, *99*, 3726−3734.
(45) Anand, B.; Majumdar, S.; Prakash, B. Structural basis unifying diverse GTP hydrolysis mechanisms. *Biochemistry* **2013**, *52*, 1122−1130.
(46) Scheidig, A. J.; Burmester, C.; Goody, R. S. The pre-hydrolysis state of p21(ras) in complex with GTP: new insights into the role of water molecules in the GTP hydrolysis reaction of ras-like proteins. *Structure* **1999**, *7*, 1311−1324.
(47) Egami, Y.; Araki, N. Dynamic Changes in the Spatiotemporal Localization of Rab21 in Live RAW264 Cells during Macropinocytosis. *PLoS One* **2009**, *4*, e6689.
(48) Fidyk, N.; Wang, J.-B.; Cerione, R. A. Influencing cellular transformation by modulating the rates of GTP hydrolysis by Cdc42. *Biochemistry* **2006**, *45*, 7750−7762.
(49) Langemeyer, L.; Bastos, R. N.; Cai, Y. Y.; Itzen, A.; Reinisch, K. M.; Barr, F. A. Diversity and plasticity in Rab GTPase nucleotide

DOI: 10.1021/acsomega.7b01025
ACS Omega 2017, 2, 6691−6702

release mechanism has consequences for Rab activation and inactivation. *eLife* **2014**, *3*, No. e01623.
(50) Bergbrede, T.; Pylypenko, E.; Rak, A.; Alexandrov, K. Structure of the extremely slow GTPase Rab6A in the GTP bound form at 1.8 Å resolution. *J. Struct. Biol.* **2005**, *152*, 235−238.
(51) Ghosh, A. P.; Marshall, C. B.; Coric, T.; Shim, E.-h.; Kirkman, R.; Ballestas, M. E.; Ikura, M.; Bjornsti, M.-A.; Sudarshan, S. Point mutations of the mTOR-RHEB pathway in renal cell carcinoma. *Oncotarget* **2015**, *6*, 17895−17910.
(52) http://cancer.sanger.ac.uk/cosmic/mutation/overview?id=3262193.

DOI: 10.1021/acsomega.7b01025
ACS Omega 2017, 2, 6691−6702